Hybrid Monomer Design for Unifying Conflicting Polymerizability/ Recyclability/Performance Properties

Changxia Shi,[1,2] Zi-Chen Li,[2] Lucia Caporaso,[3] Luigi Cavallo,[4] Laura Falivene,[3,*] and Eugene Y.-X. Chen[1,*]

[1] Department of Chemistry, Colorado State University, Fort Collins, Colorado 80523-1872, United States

[2] Beijing National Laboratory for Molecular Sciences, Key Laboratory of Polymer Chemistry and Physics of Ministry of Education, Center for Soft Matter Science and Engineering, College of Chemistry & Molecular Engineering, Peking University, Beijing 100871, China

[3] Università di Salerno, Dipartimento di Chimica e Biologia, Via Papa Paolo Giovanni II, 84100 Fisciano (SA), Italy

[4] King Abdullah University of Science and Technology (KAUST), Physical Sciences and Engineering Division, KAUST Catalysis Center, Thuwal 23955-6900, Saudi Arabia

[*]Corresponding author. Email: lafalivene@unisa.it; eugene.chen@colostate.edu

Summary: The development of intrinsically recyclable polymers promises a circular economy approach to address plastics problems including pollution and loss of their endowed energy and materials value after linear use. However, design of circular polymers is challenged by unyielding tradeoffs between monomer's polymerizability and polymer's depolymerizability and performance properties. Here we introduce a novel hybrid monomer design strategy that synergistically couples a high ceiling temperature (HCT) sub-structure for high polymerizability/performance properties with a low ceiling temperature (LCT) sub-structure for high depolymerizability/recyclability within the *same* monomer structure. Thus, structural hybridization between HCT ε-caprolactone and LCT γ-butyrolactone led to an offspring [3.2.1]bicyclic lactone (BiL), which exhibits both high polymerizability *and* depolymerizability, otherwise conflicting properties in a typical monomer. In addition, the resulting polymer (PBiL) becomes a high-performance material, with T_g up to 135 °C and T_m up to 263 °C, representing ~200 °C enhancements in both T_g and T_m relative to their parent (co)homopolymers. Furthermore, marked enhancements in PBiL's mechanical properties—10× higher Young's modulus than its parent polymers—have also been observed. These results demonstrate that the HCT/LCT hybrid monomer strategy is a powerful approach for designing circular polymers where conflicting properties must be exploited and unified.

INTRODUCTION

The current largely unsustainable plastics manufacturing, consumption, and disposal schemes have caused alarming plastics problems associated with their environmental pollution as well as tremendous energy and materials value loss in the economy.[1-4] Amongst several approaches being explored[5-16] to combat such problems, the development of next-generation, chemically recyclable polymers[17-33] promises a circular plastics economy approach to address these complex issues.[34-36] Monomer design[37,38] is the cornerstone of discovering new circular polymers with intrinsic chemical recyclability, the design of which requires to overcome typical tradeoffs between monomer's polymerizability and polymer's depolymerizability, as well as between polymer's recyclability and performance, until a practically useful balance is struck. These stringent thermodynamic, kinetic, and real-world performance requirements present a formidable challenge for developing circular plastics that exhibit not only full chemical recyclability but also high-performance properties. Nevertheless, notable advances have been achieved towards that ultimate goal. For example, the ring-opening polymerization (ROP) of low-ceiling temperature (LCT),

"nonstrained" five-membered γ-butyrolactone (γ-BL) led to poly(γ-butyrolactone) (PGBL) that can be completely depolymerized back to γ-BL in quantitative purity and yield with a low energy input.[39,40] The limited stability and mechanical performance properties of PGBL has been subsequently addressed by *trans*-fusion of a cyclohexyl ring to the γ-BL core, affording a fused bicyclic lactone monomer that led to much enhanced monomer polymerizability as well as better polymer thermal stability and crystallinity while maintaining the full chemical recyclability as a circular plastic.[21,22] However, the resulting highly crystalline polymer is a brittle material; to increase its ductility as a packaging material, synthesizing a copolymer with a sufficient amount of the flexible PGBL incorporated was required.[41] Another notable set of designer monomers for circular plastics is a class of bridged bicyclic thiolactone monomers such as chiral *N*-substituted *cis*-4-thia-L-proline thiolactones[18] and 2-thiabicyclo[2.2.1]heptan-3-one ($^{[221]}$BTL).[42] The bridged bicyclic framework locks the monomer structure in the *cis*-configuration, thus rendering the chemical recyclability and depolymerization selectivity. The classic Thorpe-Ingold effect through gem-disubstitution has also been exploited in the β-butyrothiolactone monomer design to enable the chemical recyclability.[43] Worth noting here is that the chemistry of the analogous lactones is notably different than the above thiolactones. For example, replacing the S atom in $^{[221]}$BTL with the O atom gives the bicyclic lactone congener which leads to a polyester that is atactic, amorphous, and not recyclable—essentially the opposite of the properties of the polythioester.[42]

Thus, it still remains a challenging task to combine several desired, but conflicting, properties into one lactone monomer. As copolymerization of two or more different monomers is considered as an effective strategy to obtain the materials with tailored properties by adjusting the chemical nature, composition, and sequence of the comonomers, often delivering improved or unattainable properties relative to those of the constituent homopolymers,[44-51] it thus became an attractive strategy to address the tradeoff issues. In this context, the LCT γ-BL was copolymerized with high-ceiling temperature (HCT), strained seven-membered ε-caprolactone (ε-CL)[52,53] to produce copolymers aimed for enhanced polymerizability/thermal stability and degradability/recyclability for PGBL and poly(ε-caprolactone) (PCL), respectively.[54-57] However, over the entire copolymer composition range, the glass-transition temperature (T_g, from –48 to –65 °C) and melting-transition temperature (T_m, from 11 to 63 °C) of the copolymers are still low and confined within the values of their parent homopolymers (Figure 1**A**).[58] Most recently, the comonomer strategy has been utilized to render degradability and recyclability of thermosets via incorporation of a cleavable comonomer.[59] While copolymerization can be employed as an effective strategy to mitigate the tradeoffs, increasing speciation can complicate the chemical recycling and the copolymer properties are often still confined within those of constituent homopolymers.[58]

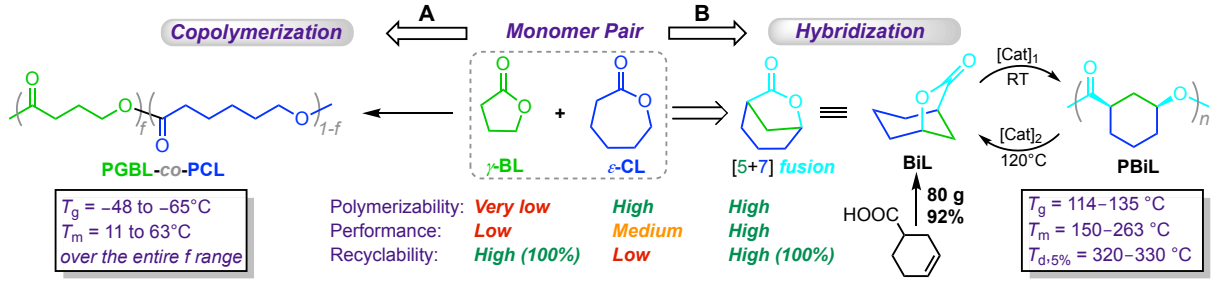

Figure 1. Hybrid monomer design vs. conventional copolymerization approach. Comparisons in monomer polymerizability as well as polymer performance and recyclability between conventional comonomer copolymerization (**A**) and new structural hybridization (**B**) strategies.

Hybridization is a common phenomenon found in chemistry and biology, the process of which combines the qualities of different varieties or species of parents to produce offspring that can be distinctively or radically different than the parents. Applying this general hybridization principle, here we introduce a novel hybrid monomer design strategy that synergistically couples a HCT sub-structure for high polymerizability/performance properties with a LCT sub-structure for high depolymerizability/recyclability within the *same* monomer structure. To demonstrate the uniqueness and effectiveness of this strategy for circular polymer design where conflicting properties must be balanced or exploited, herein we describe that *structural hybridization* between the HCT ε-CL and the LCT γ-BL leads to an offspring [3.2.1]bicyclic lactone (BiL), 6-oxabicyclo[3.2.1]octan-7-one, which can be synthesized from 3-cyclohexene-1-carboxylic acid via a two-step reaction in relatively large laboratory scale (80 g) and high yield (~92% isolated overall yield) (Figure 1**B**). We hypothesized that this hybrid monomer structure could bring about an intriguing divergent polymerization/depolymerization pathway scenario where the polymerization proceeds as if via the ring-opening of the HCT sub-structure and the depolymerization occurs as if through the ring-closing to form the LCT sub-structure (Figure 1**B**), thereby achieving both high polymerizability *and* depolymerizability, otherwise conflicting properties in a typical monomer. We further reasoned that incorporation of the cyclohexyl ring in the main chain could enhance the thermal properties of the resulting polymer.[21,60] Indeed, BiL can be readily polymerized under ambient conditions to high molecular weight poly(BiL) (PBiL) materials that exhibit both high-performance properties *and* complete chemical recyclability. Most remarkably, PBiL displays a high T_g up to 135 °C and T_m up to 263 °C, which are ~200 °C higher than both T_g and T_m values of the parent homopolymers (PGBL and PCL) and their copolymers (Figure 1**B**). In addition, mechanical properties of PBiL, particularly Young's modulus, are ~10× higher than its parent polymers, demonstrating that the HCT/LCT hybrid monomer strategy is a powerful approach for designing circular polymers and delivering radically different or drastically enhanced properties over the parent homopolymers or copolymers.

RESULTS

Suppressing epimerization to achieve exclusive stereoretention ROP

The hybrid atom-bridged bicyclic BiL is locked in a *cis*-configuration while a *trans*-configurational isomer is not possible in its monomer state. Upon the ROP, however, the resulting polymer PBiL can adopt either a *cis* (sterereoretention) or *trans* (epimerization) configurational structure, or both. Hence, our first objective was to examine whether the ROP retains the *cis*-configuration or undergoes epimerization to form a *trans*-structure and possible effects of the catalyst or mechanism on the stereorentention vs epimerization dynamics. To this end, we probed the ROP characteristics employing both organically catalyzed[61-63] and metal-catalyzed coordination-insertion mechanisms.[64,65]

As triazabicyclodecene (TBD) has been shown to be one of the most active and efficient organic catalyst for the ROP of lactones,[66,67] at the outset, we investigated characteristics of the ROP of BiL with TBD. The TBD-catalyzed ROP in toluene (6.0 M) at room temperature (RT) with [BiL]/[TBD]/[BnOH] = 600/3/1 (BnOH = benzyl alcohol as the initiator) achieved 95% conversion after 48 h. The resulting polymer PBiL had a medium number-average molecular weight (M_n) of 56.7 kg mol^{-1} but the dispersity ($Đ$) was relatively broad ($Đ$ = 1.22). NMR studies of the PBiL produced by TBD showed that *epimerization* at the carbon stereogenic center adjacent to the carbonyl carbon took place during the ROP, thus affording the PBiL containing both *cis*

(82%) and *trans* (18%) stereoconfigurations (Figure 2**A**). More specifically, the ^{1}H NMR spectrum exhibited two sets of peaks at both the alkoxy methine proton [–C*H*O–] region (labels a and a′ for *cis*- and *trans*-configurations, respectively) and the acyl methine proton [–C*H*C(C=O)–] region (labels b and b′ for *cis*- and *trans*-configurations, respectively). This finding is consistent with reports that strongly nucleophilic and basic TBD often causes side reactions during polymerization, such as transesterification and epimerization.[68] As a result, the resulting PBiL is an amorphous material but displays a high glass transition temperature (T_g) of 119 °C, as determined by differential scanning calorimetry (DSC) (Figure 2**C**). This T_g value represents ~170 – 180 °C enhancements in T_g relative to homopolymers PGBL and PCL as well as their copolymers. Noteworthy also is that it exhibits a high decomposition temperature ($T_{d,5\%}$, defined by the temperature at 5% weight loss) of 318 °C and a high maximum rate decomposition temperature (T_{max}) of 354 °C, as measured by thermogravimetric analysis (TGA) and derivative thermogravimetric analysis (DTG) (Figure 2**D**). This T_d value is about 116 °C higher than that of PGBL and similar to that of PCL.

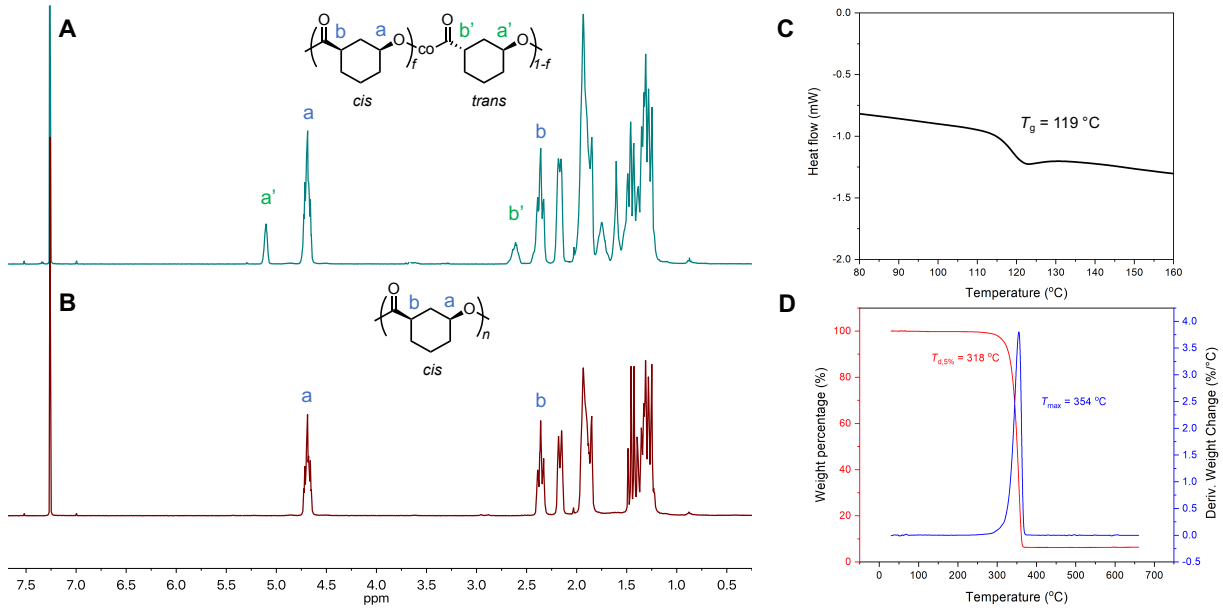

Figure 2. ^{1}H NMR (23 °C, $CDCl_3$) spectra and thermal properties of PBiL produced by organopolymerization. (**A**) PBiL produced by TBD ([BiL]/[TBD]/[BnOH] = 600/3/1), x/(x+y) = 18% (*trans* isomer derived from epimerization). (**B**) A reference PBiL produced by metal-catalyzed ROP (stereo-retention polymer product without epimerization) with La-**1** ([BiL]/[La-**1**] = 100/1). (**C**) DSC (from a second heating scan at 10 °C min^{-1}) thermogram of PBiL (M_n = 56.7 kg mol^{-1}) by TBD. (**D**) TGA and DTG (at 10 °C min^{-1} heating scan) thermograms of PBiL (M_n = 56.7 kg mol^{-1}) by TBD.

To suppress or eliminate epimerization during polymerization, next we turned our attention to the metal-mediated coordination-insertion mechanism by metal complexes bearing a vacant coordination site for binding thus activating the monomer and a nucleophilic ligand for initiating the polymerization.[64,65] As a start, we first employed La[N(SiMe$_3$)$_2$]$_3$ (La-**1**) as it is commercially available and has been shown to be highly effective for catalyzing coordination-insertion ROP of lactones[39] and also leading to cyclic polyesters when used in the absence of an alcohol co-initiator.[21] The effectiveness of La-**1** towards the ROP of BiL was examined with a [BiL]/[La-**1**]

ratio of 100/1 in toluene, achieving 96% conversion at RT after 24 h. Importantly, the PBiL produced by the metal-catalyzed coordination-insertion ROP completely returned the *cis*-configuration without noticeable racemization based on ^{1}H NMR analysis (Figure 2**B** vs. 2**A**). Specifically, the ^{1}H NMR spectrum of the PBiL produced by La-**1** displayed no peaks associated with the *trans*-configuration (i.e., a′ and b′ labeled peaks attributed to epimerization, Figure 2**B**). When combined with the co-initiator BnOH that converts instantaneously the silylamide precatalyst to the alkoxide catalyst *in situ*,[39] the polymerization at RT in toluene with [BiL]/[La-**1**]/[BnOH] = 300/1/3 achieved 92% conversion after 8 h (run 1, Table 1). The resulting polymer had a narrower dispersity of $Đ$ = 1.10 as compared to the TBD-derived PBiL.

Table 1. Results of ROP of BiL by different metal catalyst/initiator systems [a]

Run no.	Catalyst no.	[BiL]/[Cat] /[I]	Time (h)	Conv. [b] (%)	M_n(calcd)[c] (kg mol^{-1})	M_n [d] (kg mol^{-1})	$Đ$ [d] (M_w/M_n)	I* [e] (%)	Tacticity[f] (P_m)
1	La-**1**	300/1/3	8	92	11.7	13.1	1.10	90	0.35
2	*rac*-La-**2**	200/1/1	3	91	23.1	27.5	1.03	84	0.34
3	*rac*-La-**2**	1000/1/1	12	93	117	94.3	1.06	124	0.38
4	*rac*-La-**2**	1500/1/1	12	89	168	153	1.06	110	0.36
5	*rac*-Y-**1**	100/1/1	12	93	11.8	12.0	1.07	98	0.46
6	*rac*-Y-**1**	1000/1/1	16	52	65.6	59.2	1.05	111	0.52
7	*rac*-Y-**2**	100/1/1	12	86	11.0	13.4	1.05	82	0.34
8	*rac*-Y-**3**	100/1/1	72	89	11.3	10.4	1.05	84	0.42
9[g]	*rac*-Y-**3**	100/1/1	72	87	11.1	9.90	1.06	112	0.44
10	(*S,S*)-Y-**3**	100/1/1	48	65	8.43	8.90	1.06	95	0.74
11[g]	(*S,S*)-Y-**3**	100/1/1	48	52	6.67	6.70	1.05	100	0.85
12[h]	(*S,S*)-Y-**3**	100/1/1	48	46	5.92	5.60	1.09	106	0.87

[a] Conditions: $[BiL]_0$ = 6.0 M, toluene, RT, initiator (I) = BnOH (except runs 9, 11, and 12). [b] Monomer conversions measured by ^{1}H NMR of the quenched solution in benzoic acid/chloroform. [c] M_n (calculated) = ($[BiL]_0/[I]_0$) × conv.% × (molecular weight of BiL) + (molecular weight of I). [d] Weight-average molecular weights (M_w), number-average molecular weights (M_n), and dispersity indices ($Đ = M_w/M_n$) determined by gel-permeation chromatography (GPC) at 40 °C in $CHCl_3$ coupled with a DAWN HELEOS II multi (18)-angle light scattering detector and an Optilab TrEX dRI detector for absolute molecular weights. [e] Initiation efficiency (I*) = M_n(calcd)/M_n(exptl). [f] Measured by ^{13}C NMR in the carbonyl region with P_m percentages relative to the *cis*/*cis* diisotactic peak at 174.0 ppm established by the enantiomerically pure monomer. [g] (*R*)-(+)-1-Phenylethanol as initiator. [h] (*S*)-(-)-1-Phenylethanol as initiator.

The ROP of BiL by the [La-**1**] + [BnOH] system is well-controlled, as evidenced by the following *four* lines of evidence. First, the ROP followed strictly first-order kinetics (R^2 = 0.993) up to high conversions (Figure 3**A**). Second, the molecular weight increased linearly with monomer conversion while the dispersity of the resulting PBiL remained low ($Đ$ < 1.1) (Figure 3**B**). Third, the absolute molecular weight of the isolated PBiL at 92% conversion was measured by a gel-permeation chromatography (GPC) instrument equipped with multi (18)-angle light scattering and dRI (differential refractive index) detectors to have a M_n of 13.1 kg mol^{-1}; this measured M_n is close to the calculated M_n of 11.7 kg mol^{-1} based on the [BiL]/[I] ratio, thus giving a high initiation efficiency of 90% (run 1, Table 1). Furthermore, this measured M_n is essentially identical to that calculated M_n of 13.9 kg mol^{-1} based on the chain ends of PBiL characterized by ^{1}H NMR (Figure S5), which also revealed a linear chain structure and showed high end-group fidelity. Fourth, the BnOH-initiated linear structure with only the predicted end-groups, BnO–$[BiL]_n$–H, was confirmed by matrix-assisted laser desorption/ionization–time-of-flight mass spectrometry

(MALDI-TOF MS) using a low molecular weight sample prepared with [BiL]/[La-**1**]/[BnOH] = 100/1/3 (Figure 3**C**). Specifically, the MS spectrum consisted of only one series of molecular ion peaks, with the spacing between the two neighboring molecular ion peaks being that of the exact molar mass of the repeat unit (*m/z* = 126.15), as shown by the slope (126.11) of the linear plot of *m/z* values (y) *vs* the number of BiL repeat units (x) (Figure 3**D**). The intercept of the plot, 131.0, represents the total mass of chain ends + that of Na^+ [108.14 (BnO/H) + 23.0 (Na^+) g mol^{-1}].

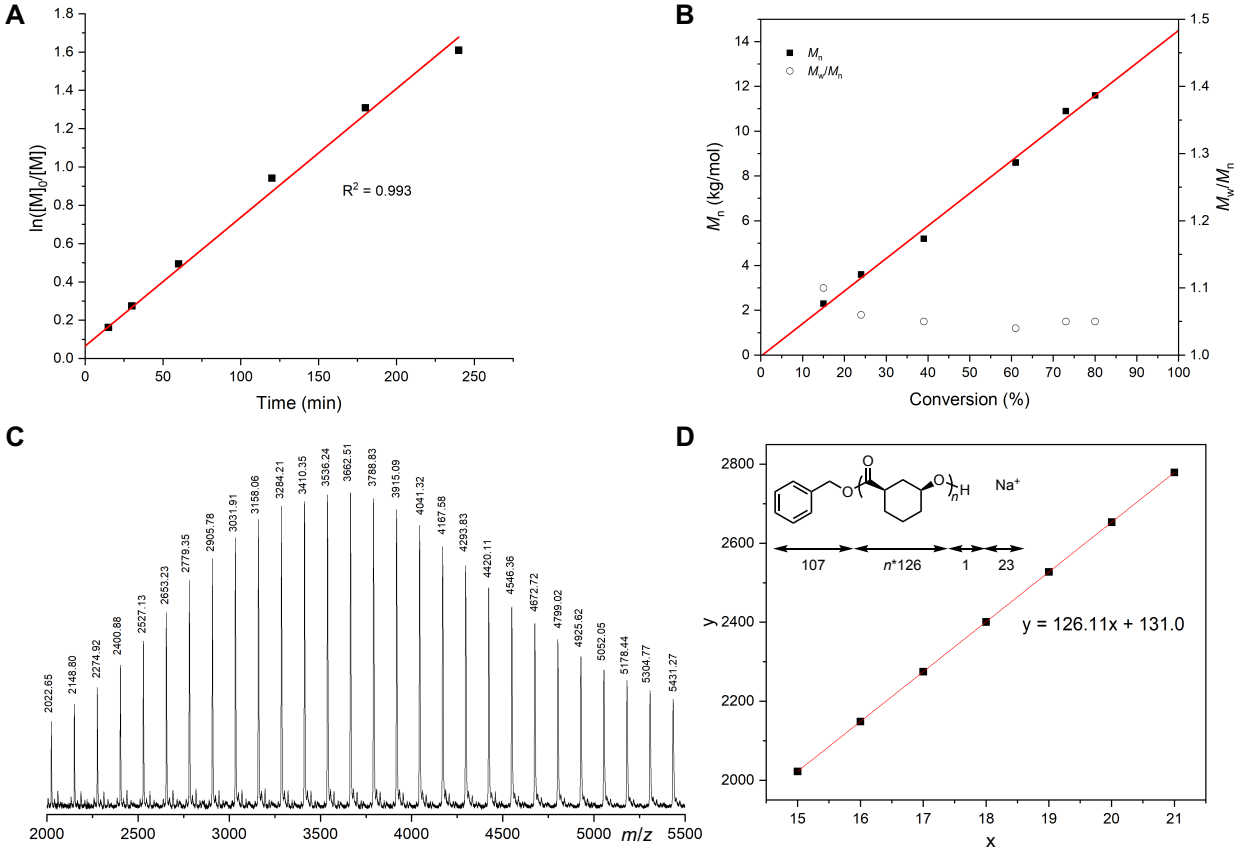

Figure 3. ^{1}H NMR (23 °C, $CDCl_3$) spectra and thermal properties of PBiL by metal-catalyzed stereoretention ROP. (**A**) Semilogarithmic kinetic plot of the ROP with [BiL]/[La-**1**]/[BnOH] = 300/1/3 ([BiL]$_0$ = 6.0 M, toluene, RT). (**B**) plots of M_n and $Đ$ values vs BiL conversion. (**C**) MALDI-TOF MS spectrum of the PBiL produced with [BiL]/[La-**1**]/[BnOH] = 100/1/3. (**D**) Plot of *m/z* values (y) *vs* the theoretical number of BiL repeat units (x).

Pure isotactic polymer from (1*R*, 5*S*)-BiL and isotactic polymer from *rac*-BiL

The above described exclusive stereoretention ROP enabled by the metal-catalyzed coordination-insertion ROP offers the opportunity to produce perfectly isotactic PBiL starting from a chiral monomer, (1*R,* 5*S*)-6-oxabicyclo[3.2.1]octan-7-one [(1*R*, 5*S*)-BiL], synthesized from commercial reagent (*R*)-(+)-3-cyclohexenecarboxylic acid. The ROP with [[(1*R*, 5*S*)-BiL]/[La-**1**]/[BnOH] = 500/1/3 yielded the corresponding chiral polymer P[(1*R*, 5*S*)-BiL] with $[\alpha]_{589}^{22.4}$ = –70 deg $dm^{-1}g^{-1}$ cm^3 in $CHCl_3$, M_n = 19.3 kg mol^{-1}, and $Đ$ = 1.08 at 94% conversion. The calculated theoretical M_n based on the [BiL]/[I] ratio is 21.1 kg/mol, which is close to both the values measured by GPC and by ^{1}H NMR (M_n = 22.5 kg mol^{-1}, Figure S7), indicating a near quantitative initiation efficiency and chain-end fidelity. The resulting polymer is a pure isotactic material, displaying *no*

stereoerrors on its ^{13}C NMR (P_m = 1.00, Figure 4**A**, Figure S8). This chiral polymer exhibited a remarkably high T_m of 293 °C on the DSC first heating scan or 263 °C on the second heating scan with a crystallization temperature of 226 °C but no observable T_g (Figure 4**B**). The semi-crystalline nature of this polymer was further confirmed by its powder X-ray diffraction (pXRD) profile, featuring sharp diffraction peaks at 2θ values of 17.3°, 18.3°, 21.5°, and 22.5°, relative to an atactic, amorphous reference PBiL sample produced from *rac*-BiL by La-**1** + BnOH (Figure 4**C**). By using La-**1** alone without the alcohol co-initiator, a chiral cyclic polymer with an ultra-high M_n of over one million Da (1,100 kg mol^{-1}, $Đ$ = 1.35) was prepared, which accordingly exhibited no end-groups (Figure S9) and stereoerrors (Figure S10).

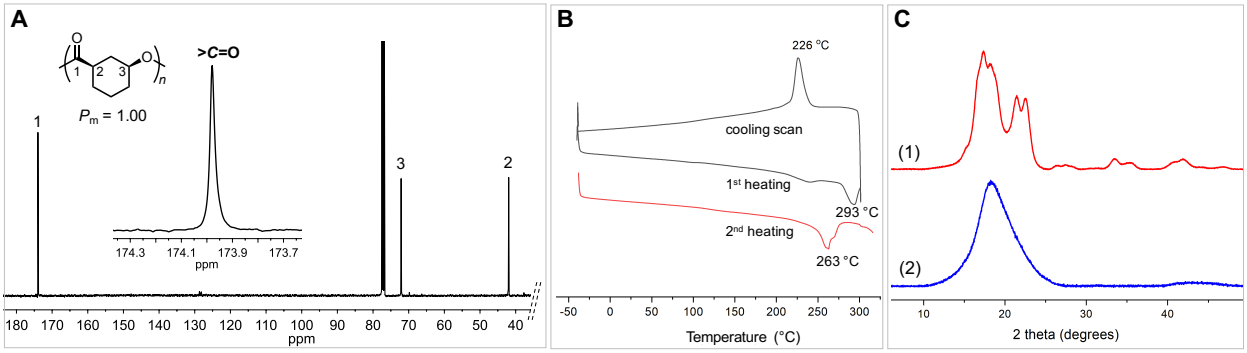

Figure 4. Pure isotactic polymer from (1*R*, 5*S*)-BiL. (**A**) ^{13}C NMR (23 °C, $CDCl_3$) spectrum of P[(1*R*, 5*S*)-BiL] prepared with [[(1*R*, 5*S*)-BiL]/[La-**1**]/[BnOH] = 500/1/3 (6.0 M, toluene, RT). (**B**) DSC thermograms of P[(1*R*, 5*S*)-BiL] from first heat, cooling, and second heating scans at 10 °C min^{-1}. (**C**) pXRD profiles of semicrystalline P[(1*R*, 5*S*)-BiL] (1) and reference amorphous PBiL derived from *rac*-BiL by La-**1** + BnOH (2).

When *rac*-BiL was polymerized by achiral catalyst La-**1**, only iso-enriched PBiL was produced with a low isotacticity of P_m = 0.35 (Figure S6). To improve the stereoselectivity of the ROP of *rac*-BiL, we next employed discrete chiral yttrium and lanthanum complexes supported by C_2-symmetric salen ligands (Figure 5**A**) as such catalysts have been shown to mediate highly stereoselective polymerization of eight-membered *rac*-diolides.[44,45,69] The use of *rac*-La-**2** supported by the sterically demanding salcy ligand with bulky CPh_3 substituents at the 3-positions of the ligand rendered much more active polymerization system but the isotacticity of PBiL remained essentially the same (runs 2-4, Table 1). However, the high activity of *rac*-La-**2**/BnOH enabled the synthesis of high-molecular-weight linear PBiL (M_n = 153 kg mol^{-1}, $Đ$ = 1.06, run 4, Table 1) by employing a high ratio of [BiL]/[*rac*-La-**2**]/[BnOH = 1500/1/1. This PBiL is an amorphous material exhibiting the highest T_g (135 °C) of the series (Figure 5**C**).

Moving to a metal center with a smaller ionic radius, *rac*-Y-**1** with 3,5-CMe_3 substituents on the salcy ligand brought about the ROP with a nearly perfect initiation efficiency (98%) and, more significantly, considerably enhanced isotacticity (P_m = 0.4, run 5, Table 1) with [BiL]/[*rac*-Y-**1**]/[BnOH] = 100/1/1. Increasing this ratio to 1000/1/1 afforded PBiL with M_n = 59.2 kg mol^{-1}, $Đ$ = 1.05, and P_m = 0.52 (run 6, Table 1). As expected, this PBiL is still an amorphous material with T_g = 128 °C. We also examined effects of solvent polarity [toluene, tetrahydrofuran (THF), dichloromethane], [BiL]/[*rac*-Y-**1**] ratio (50/1 to 300/1), and [BiL] concentration (3.0 M to 12 M) on polymerization characteristics (Table S1). Based on the results summarized in Table S1, several trends can be observed. While the ROP was fastest in THF, the resulting PBiL exhibited the

broadest dispersity (*Đ* up to 1.18). On the other hand, the ROP carried out in toluene had a moderate polymerization rate, but it produced PBiL with the narrowest dispersity. However, the tacticity of the polymer was not noticeably affected the above variations.

Further increasing the ligand steric bulk by introducing bulkier 3,5-CMe_2Ph substituents (*rac*-Y-**2**) and 3-CPh_3-5-Me substituents (*rac*-Y-**3**) to the salcy ligand did not further increase the isotacticity (runs 7 and 8, Table 1). Replacing the BnOH co-initiator with a chiral alcohol, (*R*)-(+)-1-phenylethanol, as initiator also did not noticeably affect the tacticity (run 9, Table 1). These results suggest the large amount of stereoerrors generated by these racemic catalysts could be originated from polymer chain exchange[70] between two antipodal catalyst centers (*vide infra*). To test this hypothesis, we employed enantiomeric pure catalyst (*S,S*)-Y-**3** and indeed observed a substantial increase in the polymer isotacticity to P_m = 0.74 (run 10, Table 1). When this enantiomeric catalyst was combined with a chiral alcohol co-initiator, (*R*)-(+)-1-phenylethanol or (*S*)-(-)-1-phenylethanol, the isotacticity was further increased to P_m = 0.85 (run 11, Table 1) or 0.87 (run 12, Table 1). Noteworthy also is that this high tacticity achieved was accompanied by a perfect (100%) or near perfect (106%) initiation efficiency. With this high level of isotacticity, the PBiL material derived from the stereoselective polymerization of *rac*-BiL by the chiral catalyst/initiator system finally became semi-crystalline, as evidenced by their endothermic first-order melting transitions with high T_m values at 150 °C and 154 °C (Figure 5**D**).

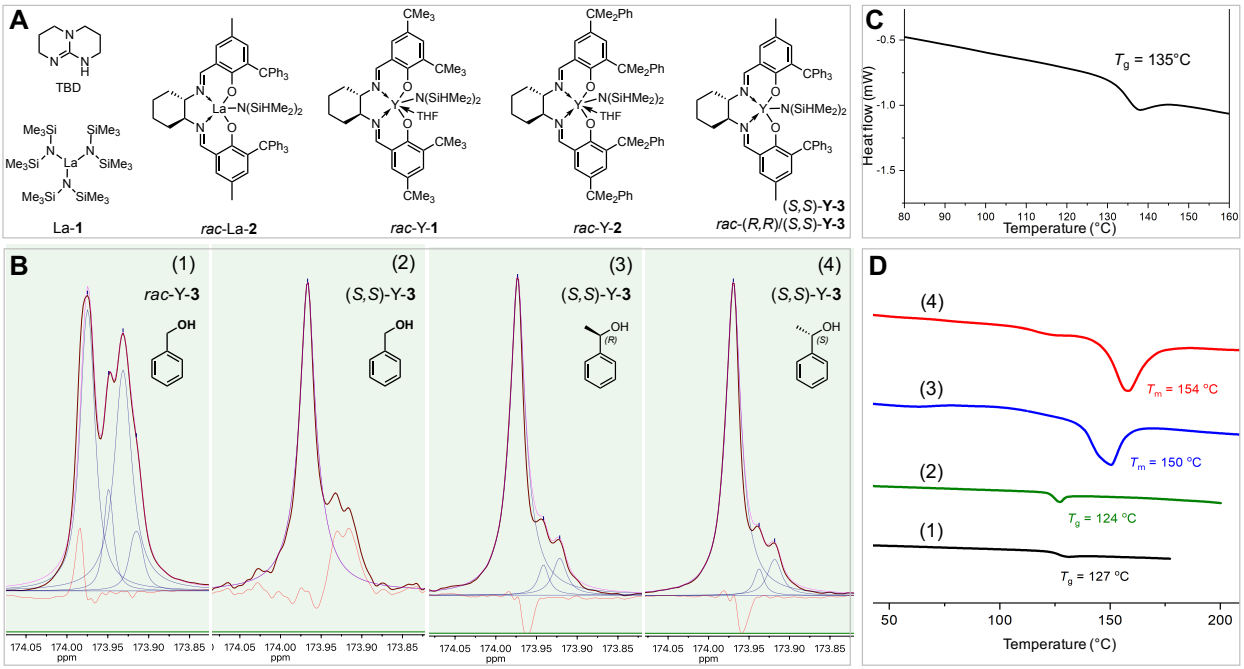

Figure 5. Iso-rich and isotactic polymers from *rac*-BiL. (**A**) Chemical structures of the catalysts employed in this study. (**B**) ^{13}C NMR (25 °C, $CDCl_3$) spectra in the carbonyl region of iso-rich (1, 2) and isotactic (3, 4) PBiL samples by racemic and enantiopure Y-**3** catalysts in combination with achiral and chiral alcohols: (1) P_m = 0.42 (run 8, Table 1); (2) P_m = 0.74 (run 10, Table 1); (3) P_m = 0.85 (run 11, Table 1); (4) P_m = 0.87 (run 12, Table 1). (**C**) DSC thermogram of the iso-rich, amorphous PBiL (M_n = 153 kg mol^{-1}, *Đ* = 1.06) by *rac*-La-**2**. (**D**) DSC thermograms of PBiL materials with varied isotacticity by racemic and enantiopure Y-**3** catalysts: (1) P_m = 0.42; (2) P_m = 0.74; (3) P_m = 0.85; (4) P_m = 0.87.

Mechanisms of stereoselection and stereoerror generation

To shed light on the mechanism of stereoselection by the enantiopure catalyst and on the generation of stereoerrors by the racemic catalyst, density functional theory (DFT) calculations were carried out first for the polymerization of BiL as a racemic mixture with (*S,S*)-Y-**3**. At the outset, we investigated the relative stability of the species comprising (*S,S*)-Y-**3** bearing a (*S,R*)-chain or a (*R,S*)-chain, namely (*S,S*)-Y-**3**/(*S,R*)-chain or (*S,S*)-Y-**3**/(*R,S*)-chain propagating sites, as a result of addition of enantiomeric monomer molecules. The DFT results showed that the (*S,S*)-Y-**3**/(*R,S*)-chain is favored by 1.5 kcal/mol, indicating a thermodynamic preference for the reactivity of (*R,S*)-BiL enantiomer with (*S,S*)-Y-**3** catalyst. Next, we investigated the kinetics of BiL insertion into the Y–O_{chain} bond to examine the effect of the monomer chirality on the interaction with the chain-end (Figure 6**A**). Starting from the more stable (*S,S*)-Y-**3**/(*R,S*)-chain propagating sites, insertion of the same enantiomer (*R,S*)-BiL is preferred over insertion of the opposite enantiomer (*S,R*)-BiL by a $\Delta\Delta G^{\ddagger}$ of 1.5 kcal/mol [activation energies for (*R,S*)-BiL and (*S,R*)-BiL insertions are 20.5 and 22.0 kcal/mol, respectively], in good agreement with the experimental P_m of 0.85. When a stereoerror occurs and a (*S,R*)-chain is formed, the resulting (*S,S*)-Y-**3**/(*S,R*)-chain site then inserts preferentially the (*S,R*)-BiL monomer over the (*R,S*)-BiL one by a $\Delta\Delta G^{\ddagger}$ of 1.2 kcal/mol [activation energies for (*R,S*)-BiL and (*S,R*)-BiL insertions are 19.1 and 17.9 kcal/mol, respectively]. Overall, these results show that, with an enantiopure catalyst, the polymerization of *rac*-BiL is moderately stereoselective through a combined catalyst-site and chain-end control mechanism, where the catalyst chirality selects the chirality of the chain and in turn the chain chirality selects the chirality of the incoming monomer, resulting in a stereoblock-like polymer structure. Any possible polymer chain exchange (*vide infra*) between the (*S,S*)-Y-**3**/(*R,S*)-chain and (*S,S*)-Y-**3**/(*S,R*)-chain sites would have no additional consequences on the polymer microstructures.

Moving to the polymerization by a racemic catalyst mixture, *rac*-Y-**3**, possible polymer chain exchange between two antipodal catalyst centers carrying opposite chains must now be taken into account. For the exchange to happen without free alcohol, we propose here a mechanism that involves an *intermolecular* transesterification step between the two enantiomers of the catalyst exchanging chains of opposite chiralities, through the formation of a dimeric intermediate (Figure 6**B**). The two anionic chain ends act as bridges between the two propagating species, while maintaining the favored seven-coordinate ligand environment typical of such Y catalysts. Out of all the possible dimeric species that could be formed, we focused on the one having opposite enantiomers of Y-**3** and opposite chiral chains, as it is the one that imposes stereomicrostructure consequences in the stereoselective polymerization as a result of polymer chain exchange. Surprisingly, this proposed dimeric intermediate (Figure 6**B**) was found to be more stable than the relative monomeric propagating species, by 2.8 kcal/mol if it dissociates as (*S,S*)-Y-**3**/(*R,S*)-chain and (*R,R*)-Y-**3**/(*S,R*)-chain, or by 5.8 kcal/mol if it dissociates as (*S,S*)-Y-**3**/(*S,R*)-chain and (*R,R*)-Y-**3**/(*R,S*)-chain, presumably due to the formation of a stabilizing Y–Y interaction (3.8 Å). This result suggests that the active site environment is mostly populated as dimers when the majority of the monomer is consumed. In this context, we have summarized the DFT results in Figure 6**B** by setting this dimeric species as a reference structure at 0 kcal/mol; the transition state for the dimer formation (Figure 6**C**) was located at 22 kcal/mol above that reference point.

Dissociation of the dimer towards the formation of higher energy monomeric (*S,S*)-Y-**3**/(*S,R*)-chain and (*R,R*)-Y-**3**/(*R,S*)-chain sites leads to more reactive but less stereoselective sites than the dissociation towards the lower energy monomeric (*S,S*)-Y-**3**/(*R,S*)-chain and (*R,R*)-Y-**3**/(*S,R*)-

chain sites, which are less reactive but more stereoselective. Specifically, the transition states for the former combination are lower in energy (17.9 and 19.1 kcal/mol) and less stereoselective ($\Delta\Delta G^{\ddagger}$ = 1.2 kcal/mol) than the latter combination, with the transition states located at higher energies (22.0 and 20.5 kcal/mol) but are more stereoselective ($\Delta\Delta G^{\ddagger}$ = 1.5 kcal/mol). Thus, in the case of polymerization by *rac*-Y-**3**, polymer chain exchange via dimeric intermediates represents an additional source of stereoerrors, as the process converts two slower and more selective propagating sites into two faster and less selective sites, thus reducing the overall stereoselectivity.

Overall, in the presence of *rac*-Y-**3**, access to the less stereoselective propagating species can occur either by polymer chain exchange, or by inherent addition/insertion errors, accounting for the additional generation of stereoerrors to produce polymers with a low P_m of ~0.45. Hence, understanding of this mechanism provides a straightforward way of enhancing the stereoselectivity by employing an enantiomeric pure catalyst, under which conditions the additional stereoerrors originated from the polymer exchange pathway are eliminated, thereby producing polymers with much higher stereoregularity (*vide supra*).

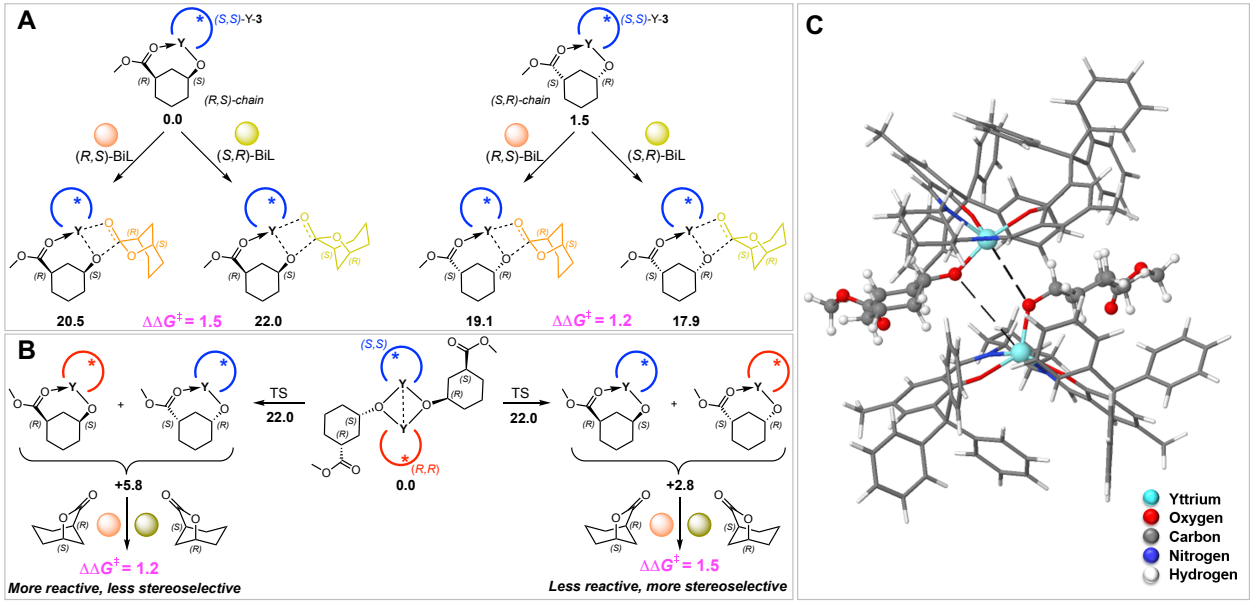

Figure 6. Summary of computational results. (**A**) Polymerization pathways and energies for the polymerization of *rac*-BiL with enantiopure (*S,S*)-Y-**3**. (**B**) Polymeric chain exchange pathway proposed for the polymerization of *rac*-BiL with *rac*-Y-**3**. (**C**) Optimized geometry of the transition state for the dimer formation along the polymer chain exchange pathway. Atoms reported as follows: Y-cyan, O-red, N-blue, C-grey, and H-white. All free energies reported in toluene and kcal/mol.

Thermal and mechanical properties and chemical recyclability

The most marked impact of structural hybridization of the LCT γ-BL with the HCT ε-CL that led to the design of the hybrid monomer BiL has been observed on thermal property enhancements. Specifically, the PBiL material derived from the [5+7] hybrid monomer BiL displays a high T_g ranging from 119 °C to 135 °C (Figures 2**C** and 5**C**), thus representing up to 200 °C enhancements in T_g relative to PGBL and PCL homopolymers as well as their copolymers. The T_m of the pure isotactic P[(1*R*, 5*S*)-BiL] was determined to be 263 °C (Figure 4**B**), also reflecting a ~200 °C increase relative to the T_m values of PGBL and PCL as well as their copolymers. The remarkable enhancement trend can be extended to the thermal stability with PBiL (with 18% *trans*) exhibiting a high $T_{d,5\%}$ of 318 °C and a high T_{max} of 354 °C (Figure 2**D**), which are about 116 °C and 136 °C higher than the $T_{d,5\%}$ and T_{max} values of PGBL. The $T_{d,5\%}$ of all *cis*-PBiL with M_n = 153 kg mol^{-1} prepared by *rac*-La-**2** (run 4, Table 1) showed a further increased $T_{d,5\%}$ to 336 °C (Figure 7**A**), approaching to that of PCL.

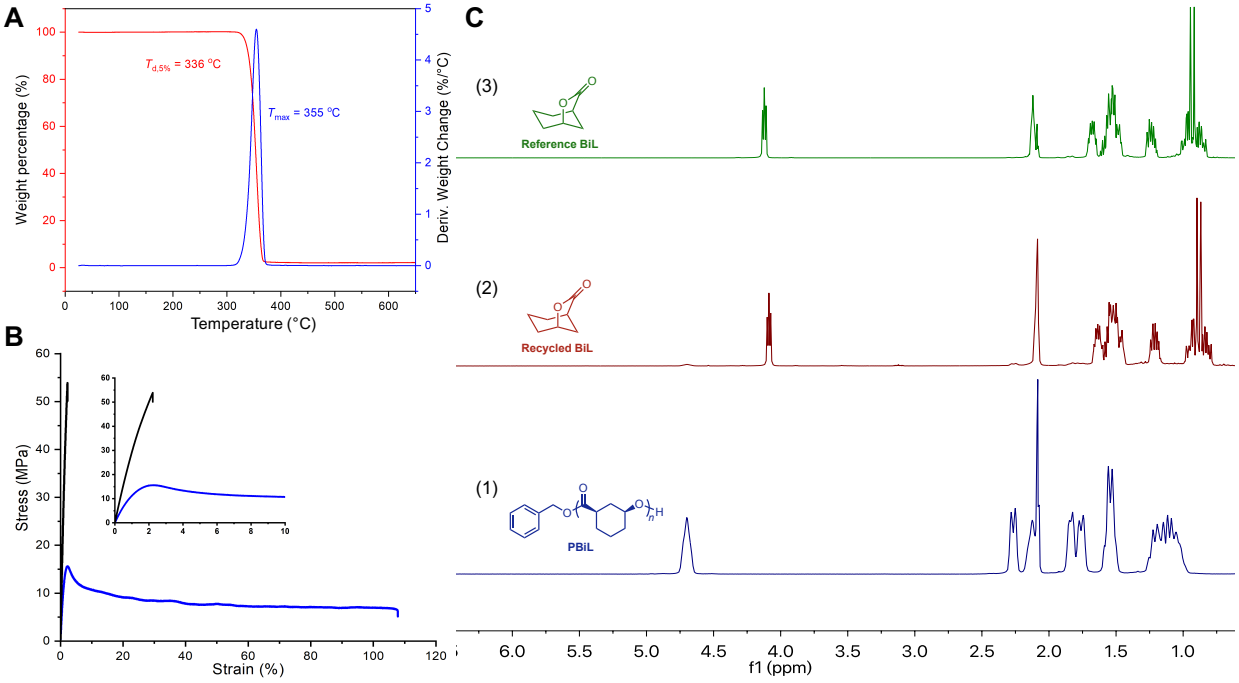

Figure 7. Thermal and mechanical properties and chemical recyclability of PBiL. (**A**) TGA and DTG thermograms of PBiL (M_n = 153 kg mol^{-1}, $Đ$ = 1.06) prepared by *rac*-La-**2**. (**B**) Stress-strain curves for the PBiL prepared by *rac*-La-**2** (M_n = 94.3 kg mol^{-1}, all *cis* structure, black curve) and the PBiL prepared by TBD (M_n = 56.7 kg mol^{-1}, *cis* (82%) and *trans* (18%) structures, blue curve). Inset: blowup region from 0 to 10% elongation. (**C**) ^{1}H NMR (toluene-d_8) spectra of PBiL (M_n = 13.1 kg mol^{-1}) prepared by La-**1** at RT (1); the recovered monomer BiL obtained after depolymerization by La-**1** at 120 °C (2); and the starting monomer BiL for comparison (3).

Mechanical properties of two PBiL samples, one with all *cis*-chains prepared by *rac*-La-**2** (M_n = 94.3 kg mol^{-1}) and the other with *cis* (82%) and *trans* (18%) prepared by TBD (M_n = 56.7 kg mol^{-1}), were examined by tensile testing of their dog-bone-shaped specimens. The all *cis*-PBiL material is best descried as a *hard*, *strong*, and *brittle* glass, as characterized by a high Young's modulus (E) = 3.05 ± 0.18 GPa, a high ultimate tensile strength (σ_B) = 53.6 ± 0.3 MPa, and a low elongation

(ε_B) = 2.2% (Figure 7**B**). As compared to PGBL (M_n = 42.5 kg mol^{-1}),[71] *cis*-PBiL enhanced the Young's modulus by ~10× and tensile strength by ~3× but with significantly reduced ductility. A similar trend was found when compared to PCL,[72] observing enhanced Young's modulus by >10× and tensile strength by ~1.5×. In contrast, the PBiL material with 18% *trans*-structure is a *plastic*, characterized by a yield point, a lower (but still high) E (2.00 ± 0.10 GPa), a lower σ_B (18.9 ± 3.3 MPa), and a higher ductility (ε_B = 85.8 ± 23.2%). Overall, these results showed that all *cis*-PBiL is drastically different than its hybridizing parents PGBL and PCL with much higher modulus but much lower ductility, and the results also demonstrated the mechanical properties of PBiL materials can be tuned by introducing some *trans*-chains via epimerization.

Another hypothesized unique feature of the HCT/LCT hybrid monomer is that it could exhibit both high polymerizability by virtue of the HCT structural motif and high depolymerizability via the LCT structural fragment, thereby unifying otherwise conflicting properties in a single monomer. To quantify the polymerizability of BiL and the depolymerizability of PBiL as a function of reaction conditions, the thermodynamics of the BiL polymerization were probed using [M]/[La-**1**]/[BnOH] = 100/1/3 (M = BiL) and $[M]_0$ = 0.5 mol L^{-1} in toluene-d_8 via a variable-temperature NMR study. The equilibrium monomer concentration, $[M]_{eq}$, obtained by plotting $[M]_t$ as a function time until [M] became constant, was measured to be 0.293, 0.216, 0.171, 0.127 and 0.0935 mol L^{-1} for 50, 40, 30, 20, and 10 °C, respectively. The van 't Hoff plot of $\ln[M]_{eq}$ vs. $1/T$ gave a straight line (R^2 = 0.999, Figures S45 and S46), from which the thermodynamic parameters were calculated to be ΔH_p^o = –21.1 kJ·mol^{-1} and ΔS_p^o = –55.8 J·mol^{-1}·K^{-1}, based on the equation $\ln[M]_{eq} = \Delta H_p^o/RT - \Delta S_p^o/R$.[53] The T_c value was calculated to be 575 K (302 °C) at $[M]_0$ = 10.0 mol L^{-1} or 379 K (106 °C) at $[M]_0$ = 1.0 mol L^{-1}, based on the equation $T_c = \Delta H_p^o/\{\Delta S_p^o + R\ln[M]_0\}$.[53] These results indicate both good polymerizability of BiL and depolymerizability of PBiL by adjusting the reaction conditions (temperature and concentration).

Consistent with the above derived thermodynamic parameters, the polymerization results summarized in Table 1 showed the relatively high polymerizability of BiL, achieving a high monomer conversion up to 93% at RT and 6.0 M of initial BiL concentration. Next, we probed the depolymerizability of the preformed PBiL by La-**1** at RT using the same catalyst at higher temperatures. Specifically, the depolymerization of PBiL in toluene-d_8 was monitored *in situ* by ^{1}H NMR, revealing that the depolymerization was complete after heating at 120 °C for 36 h to cleanly regenerate the monomer BiL (Figure 7**C**). Worth noting here is that, when the depolymerization of PBiL prepared by the TBD-catalyzed ROP at RT (M_n = 56.7 kg mol^{-1}, 82% *cis* + 18% *trans*) was performed using the same basic TBD catalyst at 120 °C, the PBiL underwent further epimerization while only a small amount of BiL was regenerated after 1 h. Nevertheless, when the depolymerization was extended to 12 h, all PBiL, including both *cis* and *trans* chains, was completely depolymerized to recover cleanly BiL (Figure S47). This exclusive selectivity for the BiL monomer recovery is possible, despite that fact that base-mediated epimerization can inter-convert the *cis* and *trans* chains, because the bridged bicyclic monomer BiL exists only in the *cis*-configuration, which is fixed by the spatially atom-bridged structure, and the monomer is stable under such base condition (in the absence of initiator). Therefore, PBiL can be completely depolymerized and converted into the most thermodynamically favored state—the monomer state under suitable conditions.

DISCUSSION

The design of useful circular polymers requires building-block monomer structures that can balance conflicting monomer polymerizability, polymer depolymerizability, and polymer performance properties. The herein described HCT/LCT hybrid monomer design synergistically utilizes both the high polymerizability and performance properties of the HCT sub-structural unit and the high depolymerizability of the LCT sub-structural unit, thereby unifying the conflicting properties in a single monomer structure. The mechanism of such hybrid monomers to solve the property tradeoffs can be thought of the intriguing two-pathway scenario where the polymerization proceeded via the ring-opening of the HCT sub-structure and the depolymerization occurred through the ring-closing to form the LCT sub-structure.

Even more intriguingly, the thermal and mechanical properties of the polymers derived from the hybridized monomers can be far superior to those homo- or copolymers of the parent monomers. This marked property enhancement has been demonstrated by the prototype example of the hybrid monomer BiL consisting of both HCT ε-CL and LCT γ-BL. Specifically on thermal properties, PBiL exhibits a high T_g up to 135 °C and T_m up to 263 °C, which are ~200 °C above both the T_g and T_m values of the parent PGBL and PCL as well as their copolymers. On mechanical properties, PBiL also showed marked enhancement in Young's modulus and tensile strength, displaying ~10× higher Young's modulus and ~3× higher tensile strength relative to PGBL, and >10× higher modulus and ~1.5× higher tensile strength relative to PCL. The HCT/LCT hybrid monomer strategy, as a powerful approach for circular polymer design which has been unequivocally demonstrated by the results reported here, should be broadly applicable to designing other monomers that can address property tradeoffs *within a single monomer structure*.

Computational studies have traced the origin of stereoerrors generated from the stereoselective polymerization of racemic BiL by both enantiopure and racemic catalysts. The derived polymer chain exchange mechanism involves the formation of the surprisingly stable dimeric propagating intermediate between the two enantiomers of the catalyst sites, which provides a pathway for exchanging the chains of opposite chiralities. Dissociation of the dimeric intermediate leads to monomeric propagating sites with more reactive/less stereoselective and less reactive/more stereoselective site combinations. With this mechanism understood, an effective strategy to eliminate such polymer-exchange-induced stereoerrors has been realized by employing a single enantiomer of the catalyst, which significantly enhanced the stereoselectivity of the polymerization.

SUPPORTING INFORMATION

The Supporting Information is available online. Experimental details, additional figures and tables (PDF, 67 pages).

ACKNOWLEDGMENT

Funding: This work was supported in part by Colorado State University and by the U.S. Department of Energy, Office of Energy Efficiency and Renewable Energy, Advanced Manufacturing Office (AMO) and Bioenergy Technologies Office (BETO). This work was performed as part of the BOTTLE™ Consortium and funded under contract no. DE-AC36-

08GO28308 with the National Renewable Energy Laboratory, operated by Alliance for Sustainable Energy. The computational study used the resources of the King Abdullah University of Science and Technology Super-Computing Laboratory (KSL). **Author contributions:** C.S. and E.Y.-X.C. conceived the idea and designed the experiments. C.S. carried out the experiments, and L.F. and L.C. performed and analyzed the DFT calculations. C.S., L.F. and E.Y-X.C. co-wrote the manuscript, and all authors participated in data analyses and discussions, read and edited the manuscript. E.Y.-X.C. directed the project. **Competing interests:** E.Y.-X.C. and C.S. are inventors on a U.S. provisional application submitted by Colorado State University Research Foundation, which covers the herein described polymers. L.C., L.F. and Z.Li declare no competing financial interests. **Data and materials availability:** All data needed to evaluate the conclusions in the paper are present in the paper and/or the Supporting Information.

REFERENCES

(1) Jambeck, J. R.; Geyer, R.; Wilcox, C.; Siegler, T. R.; Perryman, M.; Andrady, A.; Narayan, R.; Law, K. L., Plastic waste inputs from land into the ocean. *Science* **2015**, *347*, 768-771.

(2) Geyer, R.; Jambeck, J. R.; Law, K. L., Production, use, and fate of all plastics ever made. *Sci. Adv*. **2017**, *3*, e1700782.

(3) Lamb, J. B.; Willis, B. L.; Fiorenza, E. A.; Couch, C. S.; Howard, R.; Rader, D. N.; True, J. D.; Kelly, L. A.; Ahmad, A.; Jompa, J.; Harvell, C. D., Plastic waste associated with disease on coral reefs. *Science* **2018**, *359*, 460-462.

(4) World Economic Forum, Ellen MacArthur Foundation and McKinsey & Company, The new. plastics economy: Rethinking the future of plastics (2016); www.ellenmacarthurfoundation.org/ publications/the-new-plasticseconomy-rethinking-the-future-of-plastics.

(5) Report of the Basic Energy Sciences Roundtable on Chemical Upcycling of Polymers, April 30–May 1, 2019 (released in February 2020). https://science.osti.gov/-/media/bes/pdf/reports/2020/Chemical_Upcycling_Polymers.pdf.

(6) National Academies of Sciences, Engineering, and Medicine 2020. Closing the loop on the plastics dilemma: proceedings of a Workshop in brief. Washington, DC: The National Academies Press. https://doi.org/10.17226/25647.

(7) Scheutz, G. M.; Lessard, J. J.; Sims, M. B.; Sumerlin, B. S. Adaptable crosslinks in polymeric materials: Resolving the intersection of thermoplastics and thermosets. *J. Am. Chem. Soc.* **2019**, *141*, 16181−16196.

(8) Garcia, M. J.; Robertson, L. M. The future of plastics recycling. *Science* **2017**, 358, 870–872.

(9) Hillmyer, M. A., The promise of plastics from plants. *Science* **2017**, 358, 868-870.

(10) Zhu, Y.; Romain, C.; Williams, C. K. Sustainable polymers from renewable resources. *Nature* **2016**, *540*, 354−362.

(11) Zhang, X.; Fevre, M.; Jones, G. O.; Waymouth, R. M. Catalysis as an enabling science for sustainable polymers. *Chem. Rev.* **2018**, *118*, 839−885.

(12) Rorrer, N. A.; Nicholson, S.; Carpenter, A.; Biddy, M. J.; Grundl, N. J.; Beckham, G. T. Combining reclaimed PET with bio-based monomers enables plastics upcycling, *Joule* **2019**, *3*, 1006−1027.

(13) Yoshida, S.; Hiraga, K.; Takehana, T.; Taniguchi, I.; Yamaji, H.; Maeda, Y.; Toyohara, K.; Miyamoto, K.; Kimura, Y.; Oda, K. A bacterium that degrades and assimilates poly(ethylene terephthalate). *Science* **2016**, *351*, 1196−1199.

(14) Tournier, V.; Topham, C. M.; Gilles, A.; David, B.; Folgoas, C.; Moya-Leclair, E.; Kamionka, E.; Desrousseaux, M. L.; Texier, H.; Gavalda, S.; Cot, M.; Guémard, E.; Dalibey, M.; Nomme, J.; Cioci, G.; Barbe, S.; Chateau, M.; André, I.; Duquesne, S.; Marty, A., An engineered PET depolymerase to break down and recycle plastic bottles. *Nature* **2020,** *580*, 216-219.
(15) Jia, X.; Qin, C.; Friedberger, T.; Guan, Z.; Huang, Z. Efficient and selective degradation of. polyethylenes into liquid fuels and waxes under mild conditions. *Sci. Adv.* **2016**, *2*, e1501591.
(16) Rahimi, A.; García, J. M., Chemical recycling of waste plastics for new materials production. *Nat. Rev. Chem.* **2017,** *1*, 0046.
(17) Schneiderman, D. K.; Hillmyer, M. A., 50th Anniversary Perspective: There is a great future in sustainable polymers. *Macromolecules* **2017,** *50*, 3733-3749.
(18) Lu, X.-B.; Liu, Y.; Zhou, H., Learning Nature: Recyclable monomers and polymers. *Chem. Eur. J.* **2018,** *24*, 11255-11266.
(19) Jehanno, C.; Pérez-Madrigal, M. M.; Demarteau, J.; Sardon, H.; Dove, A. P., Organocatalysis for depolymerisation. *Polym. Chem.* **2019,** *10*, 172-186.
(20) Tang, X.; Chen, E. Y. X., Toward infinitely recyclable plastics derived from renewable cyclic esters. *Chem.* **2019,** *5*, 284-312.
(21) Zhu, J.-B.; Watson, E. M.; Tang, J.; Chen, E. Y.-X., A synthetic polymer system with repeatable chemical recyclability. *Science* **2018,** *360*, 398-403.
(22) Zhu, J.-B.; Chen, E. Y.-X., Catalyst-Sidearm-Induced Stereoselectivity Switching in Polymerization of a Racemic Lactone for Stereocomplexed Crystalline Polymer with a Circular Life Cycle. *Angew. Chem. Int. Ed.* **2019**, *58*, 1178-1182.
(23) Shi, C.-X.; Guo, Y.-T.; Wu, Y.-H.; Li, Z.-Y.; Wang, Y.-Z.; Du, F.-S.; Li, Z.-C., Synthesis and controlled organobase-catalyzed ring-opening polymerization of morpholine-2,5-dione derivatives and monomer recovery by acid-catalyzed degradation of the polymers. *Macromolecules* **2019,** *52*, 4260-4269.
(24) MacDonald, J. P.; Shaver, M. P., An aromatic/aliphatic polyester prepared via ring-opening polymerisation and its remarkably selective and cyclable depolymerisation to monomer. *Polym. Chem.* **2016,** *7*, 553-559.
(25) Yuan, J.; Xiong, W.; Zhou, X.; Zhang, Y.; Shi, D.; Li, Z.; Lu, H., 4-hydroxyproline-derived sustainable polythioesters: Controlled ring-opening polymerization, complete recyclability, and facile functionalization. *J. Am. Chem. Soc.* **2019**, *141*, 4928-4935.
(26) Lloyd, E. M.; Lopez Hernandez, H.; Feinberg, A. M.; Yourdkhani, M.; Zen, E. K.; Mejia,E. B.; Sottos, N. R.; Moore, J. S.; White, S. R., Fully recyclable metastable polymers and composites. *Chem. Mater.* **2019**, *31*, 398-406.
(27) Kaitz, J. A.; Lee, O. P.; Moore, J. S., Depolymerizable polymers: Preparation, applications, and future outlook. *MRS Commun.* **2015**, *5*, 191-204.
(28) Christensen, P. R.; Scheuermann, A. M.; Loeffler, K. E.; Helms, B. A. Closed-loop recycling of plastics enabled by dynamic covalent diketoenamine bonds, *Nat. Chem.* **2019**, *11*, 442−448.
(29) Garcia, J. M.; Jones, G. O.; Virwani, K.; McCloskey, B. D.; Boday, D. J.; ter Huurne, G. M.; Horn, H. W.; Coady, D. J.; Bintaleb, A. M.; Alabdulrahman, A. M. S.; Alsewailem, F.; Almegren H. A. A.; Hedrick, J. L. Recyclable, strong thermosets and organogels via paraformaldehyde condensation with diamines. *Science* **2014**, *344*, 732−735.

(30) Liu, Y.; Zhou, H.; Guo, J.-Z.; Ren, W.-M.; Lu, X.-B. Completely recyclable monomers and polycarbonate: approach to sustainable polymers. *Angew. Chem. Int. Ed.* **2017**, *56*, 4862−4866.
(31) Lizundia, E.; Makwana, V. A.; Larrañaga, A.; Vilas, J. L.; Shaver, M. P. Thermal, structural and degradation properties of an aromatic–aliphatic polyester built through ring-opening polymerisation. *Polym. Chem.* **2017**, *8*, 3530−3538.
(32) Schneiderman, D. K.; Vanderlaan, M. E.; Mannion, A. M.; Panthani, T. R.; Batiste, D. C.; Wang, J. Z.; Bates, F. S.; Macosko, C. W.; Hillmyer, M. A. Chemically recyclable biobased polyurethanes. *ACS Macro. Lett.* **2016**, *5*, 515−518.
(33) Diesendruck, C. E.; Peterson, G. I.; Kulik, H. J.; Kaitz, J. A.; Mar, B. D.; May, P. A.; White, S. R.; Martínez, T. J.; Boydston, A. J.; Moore, J. S. Mechanically triggered heterolytic unzipping of a low-ceiling-temperature polymer. *Nat. Chem.* **2014**, *6*, 623–628.
(34) Hong, M.; Chen, E. Y. X., Chemically recyclable polymers: a circular economy approach to sustainability. *Green Chem.* **2017,** *19*, 3692-3706.
(35) Hong, M.; Chen, E. Y. X., Future Directions for Sustainable Polymers. *Trends Chem.* **2019,** *1*, 148-151.
(36) Coates, G. W.; Getzler, Y. D. Y. L., Chemical recycling to monomer for an ideal, circular polymer economy. *Nat. Rev. Mater.* **2020**, *5*, 501−516.
(37) Olsén, P.; Odelius, K.; Albertsson, A.-C., Thermodynamic presynthetic considerations for ring-opening polymerization. *Biomacromolecules* **2016,** *17*, 699-709.
(38) Schneiderman, D. K.; Hillmyer, M. A., Aliphatic polyester block polymer design. *Macromolecules* **2016,** *49*, 2419-2428.
(39) Hong, M.; Chen, E. Y. X., Completely recyclable biopolymers with linear and cyclic topologies via ring-opening polymerization of γ-butyrolactone. *Nat. Chem.* **2016,** *8*, 42-49.
(40) Hong, M.; Chen, E. Y.-X., Towards Truly sustainable polymers: A metal-free recyclable polyester from biorenewable non-strained γ-butyrolactone. *Angew. Chem. Int. Ed.* **2016,** *55*, 4188-4193.
(41) Sangroniz, A.; Zhu, J.-B.; Tang, X.; Etxeberria, A.; Chen, E. Y. X.; Sardon, H., Packaging materials with desired mechanical and barrier properties and full chemical recyclability. *Nat. Commun.* **2019,** *10*, 3559.
(42) Shi, C.; McGraw, M. L.; Li, Z.-C.; Cavallo, L.; Falivene, L.; Chen, E. Y.-X. High-Performance Pan-Tactic Polythioesters with Intrinsic Crystallinity and Chemical Recyclability, *Sci. Adv.* **2020**, *6*, eabc0495.
(43) Xiong, W.; Chang, W.; Shi, D.; Yang, L.; Tian, Z.; Wang, H.; Zhang, Z.; Zhou, X.; Chen, E.-Q.; Lu, H., Geminal dimethyl substitution enables controlled polymerization of penicillamine-derived β-thiolactones and reversed depolymerization. *Chem.* **2020,** *6*, 1831-1843.
(44) Tang, X.; Westlie, A. H.; Watson, E. M.; Chen, E. Y.-X., Stereosequenced crystalline polyhydroxyalkanoates from diastereomeric monomer mixtures. *Science* **2019,** *366*, 754-758.
(45) Tang, X.; Westlie, A. H.; Caporaso, L.; Cavallo, L.; Falivene, L.; Chen, E. Y.-X., Biodegradable polyhydroxyalkanoates by stereoselective copolymerization of racemic diolides: stereocontrol and polyolefin-like properties. *Angew. Chem. Int. Ed.* **2020**, *59*, 7881−1890.
(46) Xu, Y.-C.; Ren, W.-M.; Zhou, H.; Gu, G.-G.; Lu, X.-B., Functionalized polyesters with tunable degradability prepared by controlled ring-opening (co)polymerization of lactones. *Macromolecules* **2017,** *50*, 3131-3142.

(47) Wilson, J. A.; Hopkins, S. A.; Wright, P. M.; Dove, A. P., Synthesis of ω-pentadecalactone copolymers with independently tunable thermal and degradation behavior. *Macromolecules* **2015,** *48*, 950-958.
(48) Hakkarainen, M.; Höglund, A.; Odelius, K.; Albertsson, A.-C., Tuning the release rate of acidic degradation products through macromolecular design of caprolactone-based copolymers. *J. Am. Chem. Soc.* **2007,** *129*, 6308-6312.
(49) Tabata, Y.; Abe, H., Synthesis and Properties of alternating copolymers of 3-hydroxybutyrate and lactate units with different stereocompositions. *Macromolecules* **2014,** *47*, 7354-7361.
(50) Wilson, J. A.; Hopkins, S. A.; Wright, P. M.; Dove, A. P., Dependence of copolymer sequencing based on lactone ring size and ε-substitution. *ACS Macro Lett.* **2016,** *5*, 346-350.
(51) Wilson, J. A.; Hopkins, S. A.; Wright, P. M.; Dove, A. P., Synthesis and postpolymerization modification of one-pot ω-pentadecalactone block-like copolymers. *Biomacromolecules* **2015,** *16*, 3191-3200.
(52) Labet, M.; Thielemans, W., Synthesis of polycaprolactone: a review. *Chem. Soc. Rev.* **2009,** *38*, 3484-3504.
(53) Duda, A.; Kowalski, A. in *Handbook of ring-opening polymerization*. Eds. Dubois, P., Coulembier, O. & Raquez, J.-M. Ch. 1, 1–51, Wiley-VCH, 2009.
(54) He, F.; Li, S.; Garreau, H.; Vert, M.; Zhuo, R., Enzyme-catalyzed polymerization and degradation of copolyesters of ε-caprolactone and γ-butyrolactone. *Polym.* **2005,** *46*, 12682-12688.
(55) Agarwal, S.; Xie, X., SmI_2/Sm-based γ-buyrolactone−ε-caprolactone copolymers: microstructural characterization using one- and two-dimensional NMR spectroscopy. *Macromolecules* **2003,** *36*, 3545-3549.
(56) Du, G.; Wei, Y.; Zhang, W.; Dong, Y.; Lin, Z.; He, H.; Zhang, S.; Li, X., Bis(imino)diphenylamido rare-earth metal dialkyl complexes: synthesis, structure, and catalytic activity in living ring-opening ε-caprolactone polymerization and copolymerization with γ-butyrolactone. *Dalton Trans.* **2013,** *42*, 1278-1286.
(57) Duda, A.; Penczek, S.; Dubois, P.; Mecerreyes, D.; Jérôme, R., Oligomerization and copolymerization of γ-butyrolactone — a monomer known as unable to homopolymerize, 1. Copolymerization with ε-caprolactone. *Macromol. Chem. Phys.* **1996,** *197*, 1273-1283.
(58) Hong, M.; Tang, X.; Newell, B. S.; Chen, E. Y. X., "Nonstrained" γ-butyrolactone-based copolyesters: Copolymerization characteristics and composition-dependent (thermal, eutectic, cocrystallization, and degradation) properties. *Macromolecules* **2017,** *50*, 8469-8479.
(59) Shieh, P.; Zhang, W.; Husted, K. E. L.; Kristufek, S. L.; Xiong, B.; Lundberg, D. J.; Lem, J.; Veysset, D.; Sun, Y.; Nelson, K. A.; Plata, D. L.; Johnson, J. A., Cleavable comonomers enable degradable, recyclable thermoset plastics. *Nature* **2020**, *583*, 542-547.
(60) Yu, X.; Jia, J.; Xu, S.; Lao, K. U.; Sanford, M. J.; Ramakrishnan, R. K.; Nazarenko, S. I.; Hoye, T. R.; Coates, G. W.; DiStasio, R. A., Unraveling substituent effects on the glass transition temperatures of biorenewable polyesters. *Nat. Commun.* **2018,** *9*, 2880.
(61) Kamber, N. E.; Jeong, W.; Waymouth, R. M.; Pratt, R. C.; Lohmeijer, B. G. G.; Hedrick, J. L., Organocatalytic ring-opening polymerization. *Chem. Rev.* **2007,** *107*, 5813-5840.
(62) Kiesewetter, M. K.; Shin, E. J.; Hedrick, J. L.; Waymouth, R. M., Organocatalysis: Opportunities and challenges for polymer synthesis. *Macromolecules* **2010,** *43*, 2093-2107.
(63) Dove, A. P., Organic catalysis for ring-opening polymerization. *ACS Macro Lett.* **2012,** *1*, 1409-1412.

(64) Chen, E. Y. X., Coordination polymerization of polar vinyl monomers by single-site metal catalysts. *Chem. Rev.* **2009,** *109*, 5157-5214.
(65) O'Keefe, B. J.; Hillmyer, M. A.; Tolman, W. B., Polymerization of lactide and related cyclic esters by discrete metal complexes. *J. Chem. Soc., Dalton Trans.* **2001**, 2215-2224.
(66) Pratt, R. C.; Lohmeijer, B. G. G.; Long, D. A.; Waymouth, R. M.; Hedrick, J. L., Triazabicyclodecene: A simple bifunctional organocatalyst for acyl transfer and ring-opening Polymerization of cyclic esters. *J. Am. Chem. Soc.* **2006,** *128*, 4556-4557.
(67) Chuma, A.; Horn, H. W.; Swope, W. C.; Pratt, R. C.; Zhang, L.; Lohmeijer, B. G. G.; Wade, C. G.; Waymouth, R. M.; Hedrick, J. L.; Rice, J. E., The reaction mechanism for the organocatalytic ring-opening polymerization of l-lactide using a guanidine-based catalyst: Hydrogen-bonded or covalently bound? *J. Am. Chem. Soc.* **2008,** *130*, 6749-6754.
(68) Zhang, X.; Jones, G. O.; Hedrick, J. L.; Waymouth, R. M., Fast and selective ring-opening polymerizations by alkoxides and thioureas. *Nat. Chem.* **2016,** *8*, 1047-1053.
(69) Tang, X.; Chen, E. Y. X., Chemical synthesis of perfectly isotactic and high melting bacterial poly(3-hydroxybutyrate) from bio-sourced racemic cyclic diolide. *Nat. Commun.* **2018,** *9*, 2345.
(70) Ovitt, T. M.; Coates, G. W., Stereochemistry of lactide polymerization with chiral catalysts: new opportunities for stereocontrol using polymer exchange mechanisms. *J. Am. Chem. Soc.* **2002**, *124*, 1316-1326.
(71) Zhang, C.-J.; Hu, L.-F.; Wu, H.-L.; Cao, X.-H.; Zhang, X.-H., Dual organocatalysts for highly active and selective synthesis of linear poly(γ-butyrolactone)s with high molecular weights. *Macromolecules* **2018,** *51*, 8705-8711.
(72) Moore, T.; Adhikari, R.; Gunatillake, P., Chemosynthesis of bioresorbable poly(γ-butyrolactone) by ring-opening polymerisation: a review. *Biomaterials* **2005,** *26*, 3771-3782.